HZDR-050

EMITTANCE MINIMIZATION AT THE ELBE SUPERCONDUCTING ELECTRON GUN

K. Möller, A. Arnold, P. Lu, P. Murcek, J. Teichert, H. Vennekate, R. Xiang

Wissenschaftlich-Technische Berichte
HZDR-050 · ISSN 2191-8708

WISSENSCHAFTLICH-
TECHNISCHE BERICHTE

HZDR
HELMHOLTZ
ZENTRUM DRESDEN
ROSSENDORF

Wissenschaftlich-Technische Berichte
HZDR-050

K. Möller, A. Arnold, P. Lu,
P. Murcek, J. Teichert, H. Vennekate, R. Xiang

EMITTANCE MINIMIZATION AT THE ELBE SUPERCONDUCTING ELECTRON GUN

HZDR
HELMHOLTZ
ZENTRUM DRESDEN
ROSSENDORF

Druckausgabe: ISSN 2191-8708

Elektronische Ausgabe: ISSN 2191-8716

Qucosa: http://fzd.qucosa.de/startseite/

2014

Herausgegeben vom

Helmholtz-Zentrum Dresden - Rossendorf

Bautzner Landstr. 400

01328 Dresden

Germany

Emittance Minimization at the ELBE Superconducting Electron Gun

K. Möller, A. Arnold, P. Lu, P. Murcek, J. Teichert, H. Vennekate, R. Xiang FWKE

Zusammenfassung

Die transversale Emittanz ist eine der wichtigsten Größen, welche die Qualität einer Elektronenquelle charakterisieren. Für hochqualitative Experimente werden Strahlen niedriger Emittanz benötigt. Mit Hilfe theoretischer Betrachtungen und Computersimulationen wurde untersucht, wie sich die Emittanz der Rossendorfer supraleitenden Hochfrequenz-Fotoelektronenquelle (SRF-Gun) minimieren lässt.

Es stellte sich heraus, dass weder ein Solenoid-Magnet noch Raumladungskräfte benötigt werden um ein deutliches Minimum der Emittanz zu erzeugen. Das Emittanzminimum tritt auf, wenn die Startphase des Elektronenpulses bezüglich der HF-Phase in geeigneter Weise gewählt wird.

Die Untersuchung unterschiedlicher Korrelationen zwischen den Eigenschaften der Strahlteilchen führt zu einer Erklärung wie das Minimum entsteht. Es wird nachgewiesen, dass der Hauptgrund für ein Minimum darin zu suchen ist, dass die longitudinalen Eigenschaften der Strahlteilchen (Energie) stark durch die Startphase beeinflusst werden. Infolge der Kopplung zwischen den longitudinalen und transversalen Freiheitsgraden in der relativistischen Bewegungsgleichung können die transversalen Freiheitsgrade und damit auch die Emittanz gleichfalls durch die Startphase stark mitbestimmt werden. Die Ergebnisse dieser Studie werden verwendet um die Emittanz der SRF-Gun während der Inbetriebnahme und Optimierungsphase zu minimieren.

Summary

The transverse emittance is one of the most important quantities which characterize the quality of an electron source. For high quality experiments low beam emittance is required. By means of theoretical considerations and simulation calculations we have studied how the emittance of the Rossendorf superconducting radio-frequency photoelectron source (SRF gun) can be minimized.

It turned out that neither a solenoid magnet nor the effect of space charge forces is needed to create a pronounced emittance minimum. The minimum appears by just adjusting the starting phase of the electron bunch with respect to the RF phase of the gun in a suitable way.

Investigation of various correlations between the properties of the beam particles led to an explanation on how the minimum comes about. It is shown that the basic mechanism of minimization is the fact that the longitudinal properties of the particles (energy) are strongly influenced by the starting phase. Due to the coupling of the longitudinal and transverse degrees of freedom by the relativistic equation of motion the transverse degrees of freedom and thereby the emittance can be strongly influenced by the starting phase as well. The results obtained in this study will be applied to minimize the emittance in the commissioning phase of the SRF gun.

1. Introduction

The report deals with the behaviour of the transverse emittance of the Rossendorf superconducting radio-frequency photoelectron source (SRF gun). Details of the SRF gun design can be found in ref. [1]. The transverse emittance is one of the most important quantities which characterize the quality of an electron source.
An experimental standard setup for minimizing the emittance is shown in Fig. 1.

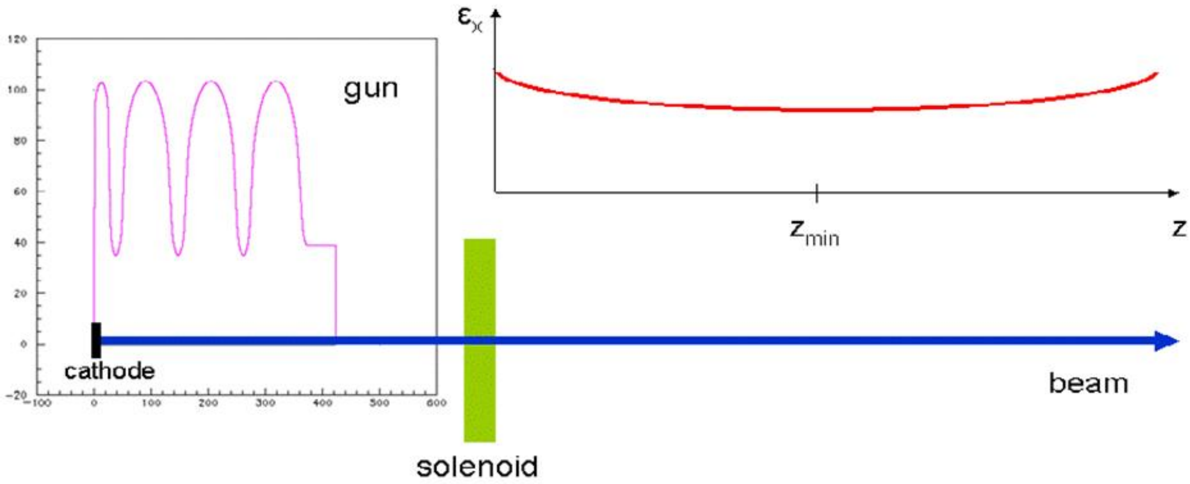

Fig. 1: Standard setup to minimize the emittance.

By changing the varies parameters in the setup like the solenoid current, the starting phase of the electron bunch, the length and the shape of the bunch, the shape of the cathode, the radius of the bunch etc. somewhere downstream behind the exit of the gun one can create an emittance minimum. This minimum is in general a shallow minimum (< 10%). Since it is not known why this minimum is appearing at all no handle is available how one can optimize the minimum systematically.
In the course of the present investigation it has been found that no solenoid is needed to generate a minimum in the z-region downstream to the exit of the gun. Furthermore it turned out that an even deeper minimum appears if the space charge forces are turned off in the simulation calculations. Thus the appearance of the minimum can be studied under very “clean” conditions since the space charge contribution introduces the biggest numerical error (up to about 10%) in the calculations. If the space charge contribution is turned off in the calculations the math in the simulation code is reduced to solving the relativistic equation motion for the particles moving in the electromagnetic cavity fields. In the simulation codes this is done with high numerical accuracy.
Once the reason of the appearance of the emittance minimum is understood in a step by step procedure different effects can be added to the “clean” conditions, like taking space charge into account by increasing the bunch charge starting from zero bunch charge. There are a lot of practical cases where small bunch charges are applied. For these cases similar condition can be assumed to hold as for zero bunch charge. In the simulation calculations it can be studied how the minimum behaves if the bunch charge is increased.

2. Simulation results for zero bunch charge

In Fig.2 the emittance behaviour is shown in the drift region behind the gun for different starting phase settings. The parameters chosen are: the maximum electric field strength in the cavity is 40 MV/m, the bunch has cylindrical shape with 2 mm radius and 15 ps length. The bunch charge equals zero. The simulations were performed with the SGUN_MOTION code [2].

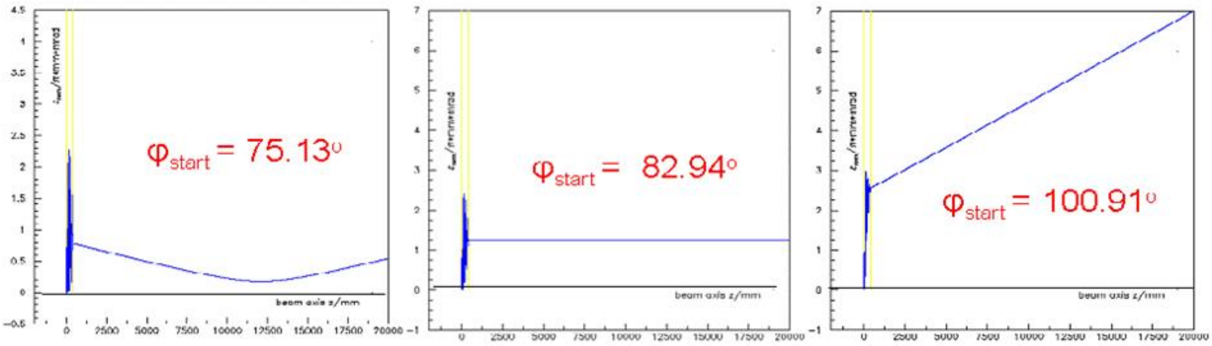

Fig. 2: Generation of an emittance minimum by suitable setting of the starting phase (no space charge forces).

It can be seen that the emittance is very sensitive to the phase. For $\phi = 75.13^{o}$ a deep minimum can be generated and for $\phi = 100.91^{o}$ a steep rise occurs.

3. Comparison with ASTRA code simulations

In this chapter the results obtained in the previous section are compared to corresponding calculations performed with the ASTRA code [3]. The results are shown in figs. 3a, 3b, and 3c correspondingly.

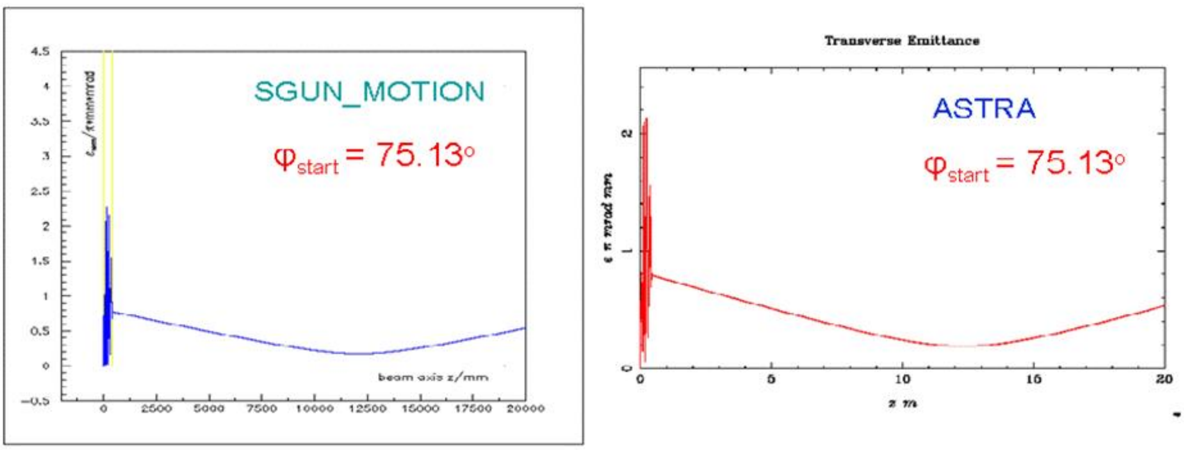

Fig. 3a: Comparison of SGUN_MOTION and ASTRA calculations for the starting phase $\varphi_{start} = 75.13^{o}$.

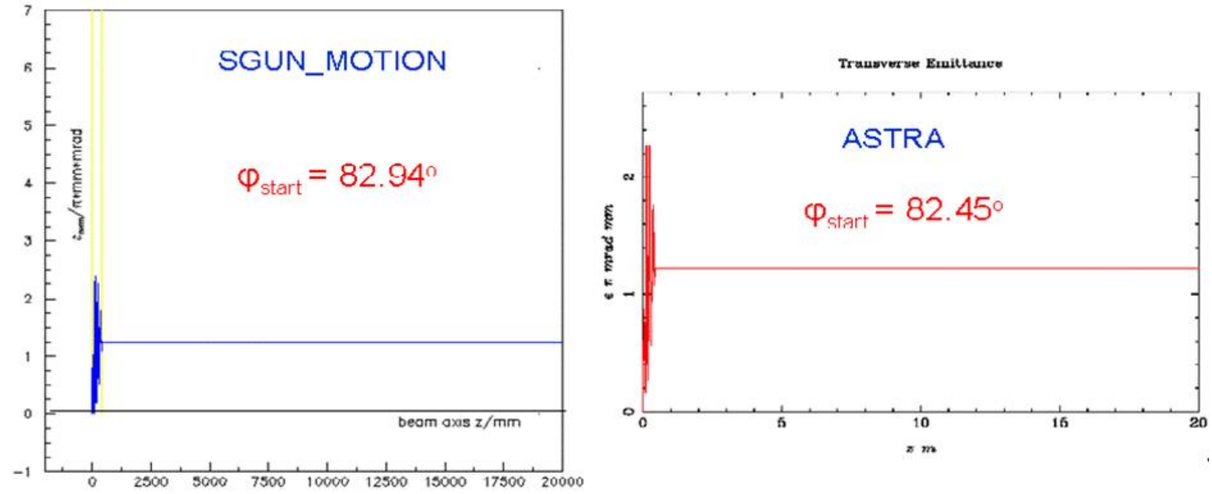

Fig. 3b: Comparison of SGUN_MOTION and ASTRA calculations for ϕ_{start} = 82.94^o and ϕ_{start} = 82.45^o respectively.

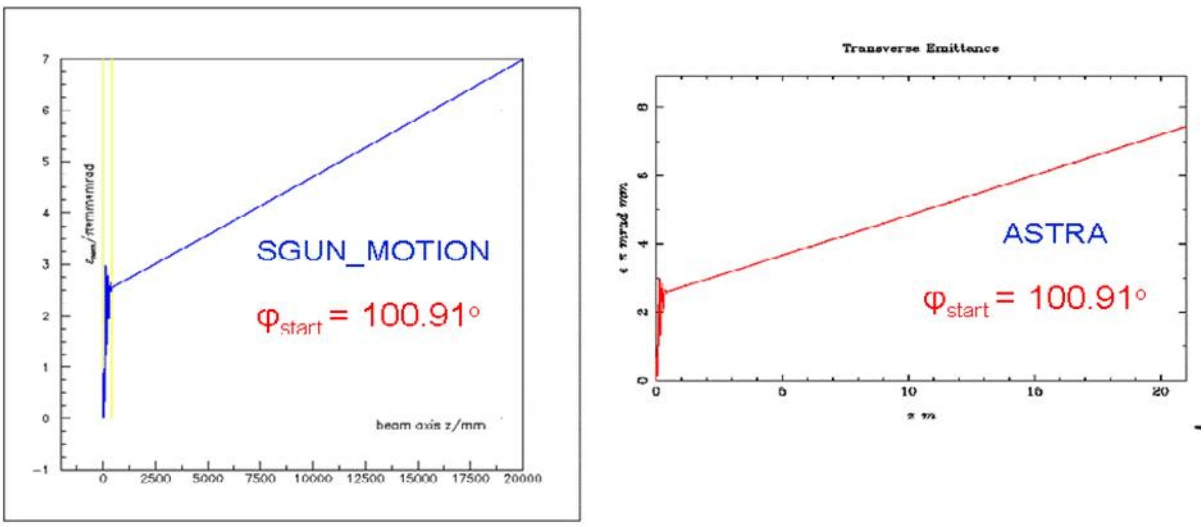

Fig. 3c: Comparison of SGUN_MOTION and ASTRA calculations for ϕ_{start} = 100.91^o.

As can be seen from these figures the results of the two simulation codes agree with a high degree of precision.

4. Theoretical study of emittance

From the theoretical point of view the emittance is, except from some calibration factor, the phase space volume occupied by the particles of the bunch in the corresponding phase space. In general to describe the beam in phase space we need to consider a 6N-dimensional phase space with N being the number of particles in the bunch. If the space charge interaction is turned off as in the present case the particles of the bunch move as independent particles and the bunch can be described in a 6-dimensional phase space.

The position of a particle in the 6-dimensional phase space can be described by the generalized vector

$$\vec{R} \equiv (\vec{r}, \vec{p}) \equiv x \cdot \vec{e}_1 + y \cdot \vec{e}_2 + z \cdot \vec{e}_3 + p_x \cdot \vec{e}_4 + p_y \cdot \vec{e}_5 + p_z \cdot \vec{e}_6 \qquad (1)$$

This vector changes in time according to

$$\begin{aligned} &\dot{\vec{R}} \equiv \frac{d\vec{R}}{dt} \equiv \vec{V} = (\dot{\vec{r}}, \dot{\vec{p}}) = \\ &\dot{x} \cdot \vec{e}_1 + \dot{y} \cdot \vec{e}_2 + \dot{z} \cdot \vec{e}_3 + \dot{p}_x \cdot \vec{e}_4 + \dot{p}_y \cdot \vec{e}_5 + \dot{p}_z \cdot \vec{e}_6 \end{aligned} \qquad (2)$$

The quantity $\vec{V}$ can be interpreted as a generalized velocity in the 6-dimensional phase space. Using the Hamilton formalism the motion of relativistic particles under the influence of electromagnetic forces can be represented in the following form

$$\begin{aligned} \dot{\vec{r}} &= \frac{\partial H(\vec{r}, \vec{p})}{\partial \vec{p}} \\ \dot{\vec{p}} &= -\frac{\partial H(\vec{r}, \vec{p})}{\partial \vec{r}} \end{aligned} \qquad (3)$$

with the Hamiltonian

$$H(\vec{r}, \vec{p}, t) = eU(\vec{r}, t) + c\sqrt{(mc)^2 + \left(\vec{p} - e\vec{A}(\vec{r}, t)\right)^2} \qquad (4)$$

The quantities U and $\vec{A}$ are the scalar and vector electromagnetic potentials respectively. For the electromagnetic forces acting in the cavity the scalar potential U is equal to zero. By inserting the Hamiltonian in the Hamilton equations and using the relations between the electromagnetic fields and the electromagnetic potentials we obtain the following well known equation of motion for relativistic particles moving under the influence of Lorentz-forces

$$\vec{F} \equiv \frac{d}{dt}\vec{q} \equiv \frac{d}{dt}\left(\vec{p} - e\vec{A}\right) = e\vec{E} + \dot{\vec{r}} \times \vec{B} \quad (Lorentz\ force) \qquad (5)$$

where

$$\vec{E} = -\frac{\partial}{\partial t}\vec{A} \ \text{ and } \ \vec{B} = \frac{\partial}{\partial \vec{r}} \times \vec{A}.$$

The momenta $\vec{q}$ and $\vec{p}$ are the mechanical and canonical momenta of the particles respectively.
Using the Hamilton equations we obtain for the generalized velocity vector

$$\vec{V} = \left(\frac{\partial H}{\partial \vec{p}}, -\frac{\partial H}{\partial \vec{r}}\right) \tag{6}$$

We define a generalized gradient in the 6-dimensional phase space by

$$\frac{\partial}{\partial \vec{R}} \equiv \left(\frac{\partial}{\partial \vec{r}}, \frac{\partial}{\partial \vec{p}}\right) \tag{7}$$

Applying this operator to the velocity field $\vec{V}(\vec{R})$ we get

$$\frac{\partial \vec{V}}{\partial \vec{R}} = \left(\frac{\partial}{\partial \vec{r}}\frac{\partial V}{\partial \vec{p}} - \frac{\partial}{\partial \vec{p}}\frac{\partial V}{\partial \vec{r}}\right) = 0 \tag{8}$$

If the particles in the phase space are distributed according to a mass density distribution $\rho\left(t, \vec{R}\right)$ from the conservation of the total mass we can deduce the continuity equation

$$\frac{\partial \rho\left(t, \vec{R}\right)}{\partial t} + \frac{\partial}{\partial \vec{R}}\left[\rho\left(t, \vec{R}\right) \cdot \vec{V}\left(t, \vec{R}\right)\right] = 0 \tag{9}$$

For an assumed space independent constant density distribution at $t = 0$

$$\rho\left(t = 0, \vec{R}\right) = \rho_0$$

we deduce with eq. (8)

$$\frac{\partial \rho_0(t)}{\partial t} + \frac{\partial}{\partial \vec{R}}\left[\rho_0(t) \cdot \vec{V}\left(t, \vec{R}\right)\right] = \frac{\partial \rho_0(t)}{\partial t} + \rho_0(t)\frac{\partial}{\partial \vec{R}}\vec{V}\left(t, \vec{R}\right) = \frac{\partial \rho_0(t)}{\partial t} = 0 \tag{10}$$

The result

$$\rho\left(t, \vec{R}\right) = \rho_0 = const \tag{11}$$

means if the density ρ is constant in space at $t = 0$ it stays constant in time. The velocity field can be interpreted as a field of an incompressible liquid.

This result means that any arbitrary closed region in the 6-dimensional phase space changes its shape in time but not its “volume” (s. Fig.4). This is just what the well known Theorem of LIOUVILLE states.

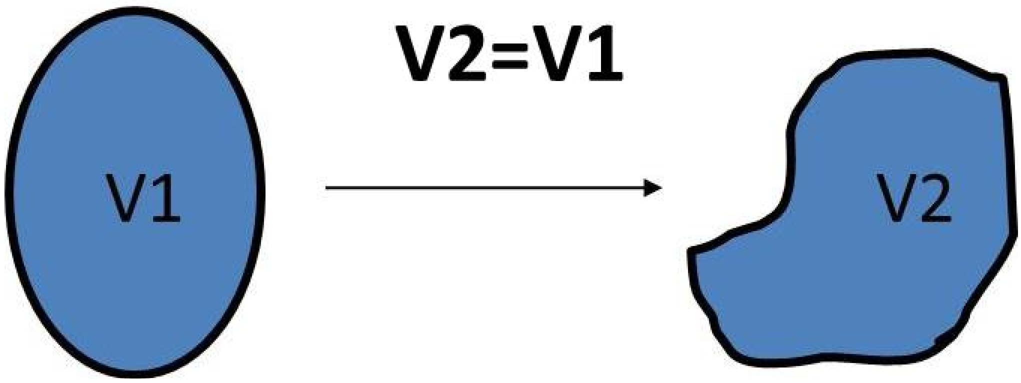

Fig. 4: Conservation of phase space volume.

5. Emittance behaviour at the exit of the gun

Next we study in detail the emittance behaviour of the SRF gun downstream of the gun exit. In this region there are no forces acting on the beam particles (i.e., a setup like in Fig.1 but without a solenoid present). The relativistic equation of motion as given in eq. (5) is then reduced to

$$\vec{F} \equiv \frac{d}{dt}\vec{q} = 0. \qquad (12)$$

With $\vec{p} \equiv \vec{q}$ we get for the momentum of particles

$$\vec{p} = \begin{pmatrix} p_x \\ p_y \\ p_z \end{pmatrix} = const. \qquad (13)$$

Rewriting the relativistic momenta in terms of the velocity components we get

$$\vec{p} = m_0\gamma\vec{v} = m_0\gamma c^2\frac{1}{c^2}\vec{v} = \frac{E(v_x, v_y, v_z)}{c^2}\vec{v} \qquad (14)$$

with $E(v_x,v_y,v_z)$ being the total energy of the particles as given by

$$E(v_x, v_y, v_z) = \frac{m_0c^2}{\sqrt{\left(1 - \frac{(v_x^2 + v_y^2 + v_z^2)}{c^2}\right)}} \qquad (15)$$

The quantity m_0 is the rest mass of the particles.

Decomposing the momentum vector into components yields

$$p_x = \frac{E(v_x, v_y, v_z)}{c^2} v_x \tag{16a}$$

$$p_y = \frac{E(v_x, v_y, v_z)}{c^2} v_y \tag{16b}$$

$$p_z = \frac{E(v_x, v_y, v_z)}{c^2} v_z \tag{16c}$$

Looking at eq. (16) we see that even for zero external forces the momenta of the three components are not unique functions of their respective velocities but depend also on the remaining velocities. This coupling is lifted only in the limit of zero velocities i.e., in the nonrelativistic limit. In this case the energy takes on the value of the rest mass of the particles $E=m_0c^2$ and the equations (16) will decouple.

The coupling of the velocity (momentum) degrees of freedom for relativistic particles originates from the relativistic mass increase if the velocity of the particles is increased. This coupling leads to the very important conclusion that the (x, p_x)-subspace in the 6-dimensional phase space (x,y,z,p_x,p_y,p_z) is not a separate subspace but is coupled to the p_y and p_z degrees of freedom in the 6-dimensional phase space. Therefore the Liouville-theorem is not valid in the (x,p_x)-subspace and the corresponding emittance ε_x is not constant. One should keep in mind that ε_x is just the quantity which is usually measured in experiments set up to determine the transverse emittance.

We want to stress that the preceding considerations are the most important features in studying and understanding the appearance of a minimum in the ε_x emittance. It is by this coupling that one can influence the transverse properties of the particles, like the emittance ε_x, by changing the longitudinal properties like v_z (and thereby the total energy E). At the exit of the gun there is a strong dependence of the transverse velocity v_x on the longitudinal velocity v_z since after acceleration v_z is very close to the velocity of light c.

Based on the presented theoretical background we will now study the ε_x emittance behaviour for the drift region in greater detail and in practical terms. We analyse the situation depicted in fig.5. Here it is assumed that the bunches are drifting along the beam axis from z_1 to z_2. Then we have to answer the question how the emittance ε_x changes by going from position z_1 to z_2. To answer this question one has to refer to the phase space plots of the bunch at the exit of the gun at position $z = z_1$ and at the position $z=z_2$ after the drift process of the bunch has occurred.

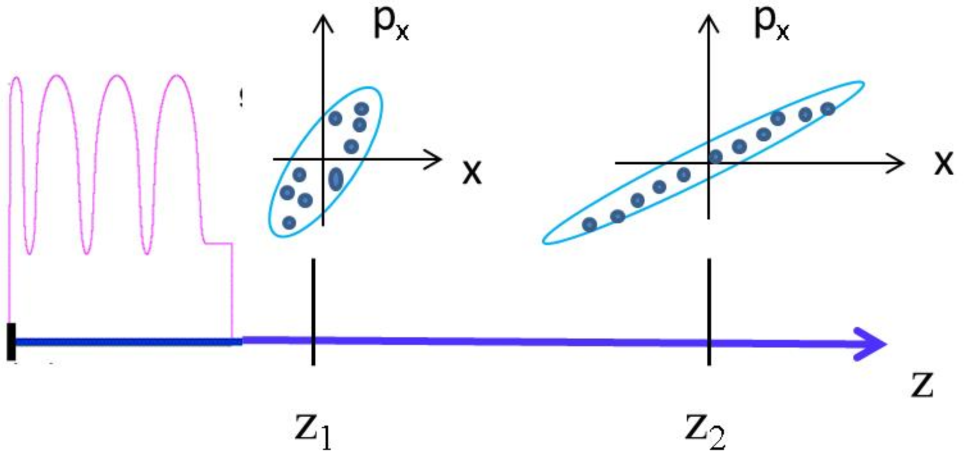

Fig. 5: Scheme for the investigation of the emittance in the drift region.

The respective values of the areas occupied by the particles in the two phase space plots determine the emittance ε_x (apart from a possible calibration factor). To answer the question whether the area of the plot has changed by the drift process we look at fig.6.

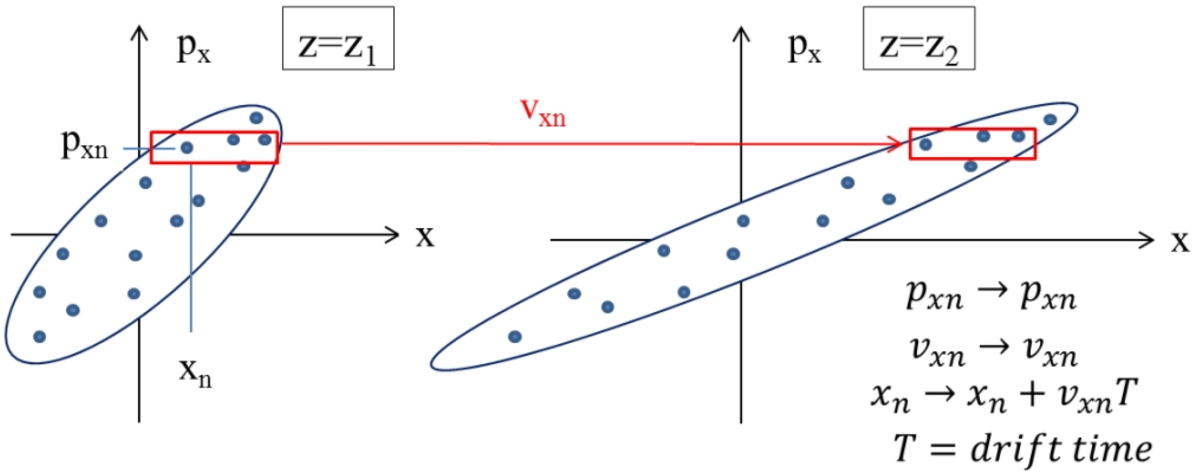

Fig.6 Details of the drift process in terms of phase space

Since according to eq.(12) through eq.(16) all momenta and all velocities of the particles stay constant to obtain the phase space plot after the drift process the particles in the left-hand plot in Fig.6 are simply shifted to the right. The shift in x-direction is given by x_p --->x_p +v_{xn}T with v_{xn} being the drift velocity v_x of particle n in x-direction.
To compare the areas of the two phase space plots in greater detail we decompose the total area of the initial plot at z=z_1 into small virtual boxes around the particles with an assumed momentum p_{xs} with some channel width Δp_x. In the simulation calculations Δp_x must be chosen wide enough to have at least a few particles in this momentum channel. By choosing a big number of particles in the bunch this requirement can always be fulfilled.
In nonrelativistic mechanics all particles contained in the box with momentum p_{xs} have the velocity $v_{xs} = p_{xs} /m_0$. Here the width of the box is assumed to be small enough so that velocity changes due to the width of the box can be neglected. Since all momenta and all velocities of the particles stay constant for the drift process the change of the phase space plot by the drift process simply comes down to shifting the respective boxes by an amount of v_{xs}T. In this case the lengths of the boxes do neither expand nor shrink. Since this is true for all boxes the whole area of the phase space plot does not change by the drift process, i.e., the emittance stays constant.
This result is true only for nonrelativistic particles. In mathematics terms this result is caused by the fact that there is a unique relation between the velocity v_x and the momentum p_x. The electrons at the exit of the gun however can not be treated as non-relativistically but are highly relativistic. Their velocity v_z in beam direction is close to the velocity of light c. In this case according to eq.(16a) the velocity v_x is no longer a unique function of p_x but for a given value of p_x the velocity v_x depends also on the total energy $E(v_x, v_y, v_z)$. This means in this indirect way v_x also depends on v_y and v_z. Here the dependence on the longitudinal velocity v_z is very strong since after acceleration v_z is very close to the velocity of light c. Therefore according to Eq.(16) it can be concluded that for a given momentum p_x the transverse velocity v_x of the particles in the bunch is strongly coupled to the longitudinal properties , i.e., to the total energy.
If this result is transferred to the picture in Fig.6 this means that inside a box, however small, there can occur particles with (slightly) different velocities. This result is corroborated by simulation calculations shown in Fig.7. Rather than having a unique relation between p_x and v_x we observe a

band of velocities whose width characterizes the range of the velocities for a given p_x. According to Eq.(16) this range reflects the range of the values of the total energy of the bunch particles.

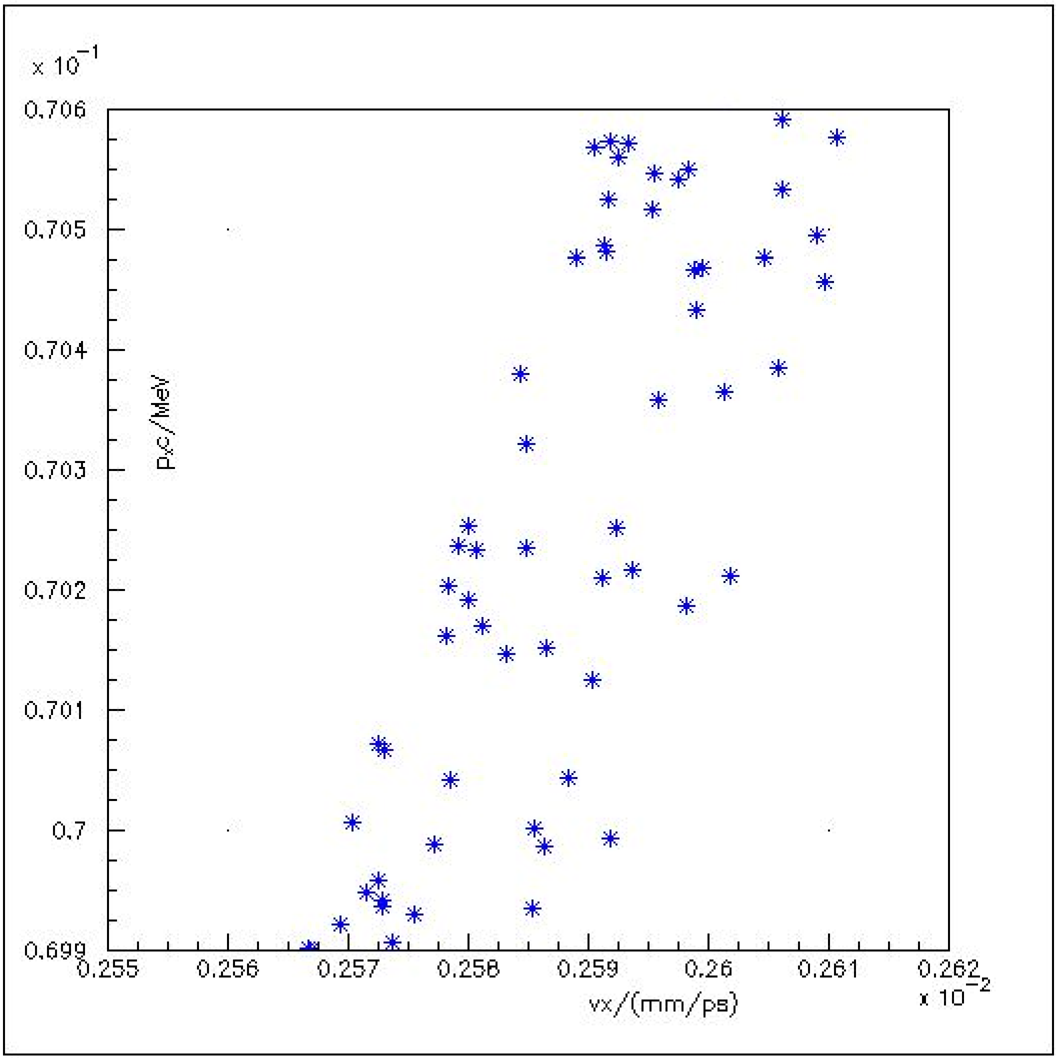

Fig.7: Band of velocities versus momentum values.

Having a range of velocities inside a box in Fig.7 leads to the fact that the boxes may change their length and thereby their area in the drift process so that the area of the whole phase space plot may change. This means the emittance will no longer be constant in the drift process. Going even further into the details one can study the correlation of the particle velocities inside a box with their position x. There are three interesting cases which can be observed in the simulation calculations:

1. The particles at larger x are faster than the ones at smaller x. This will cause the boxes to get longer in the drift process. In this case the emittance will grow.
2. If the particles at lower x-values are faster than the ones at larger x the length of the boxes will first shrink and then after the faster particles catch up with the slower ones the area of the boxes will start to rise. This scenario will lead to a minimum in the emittance curve if plotted over the beam axis z.
3. If there is no correlation between the velocity v_x and x then the emittance will stay constant. These theoretical considerations will now be corroborated by simulation results. At first in Fig.s 8a and 8b the existence of the emittance minimum at 75.13° is shown by comparing the phase space plot at position z_1 with a plot at the emittance minimum position z_2.

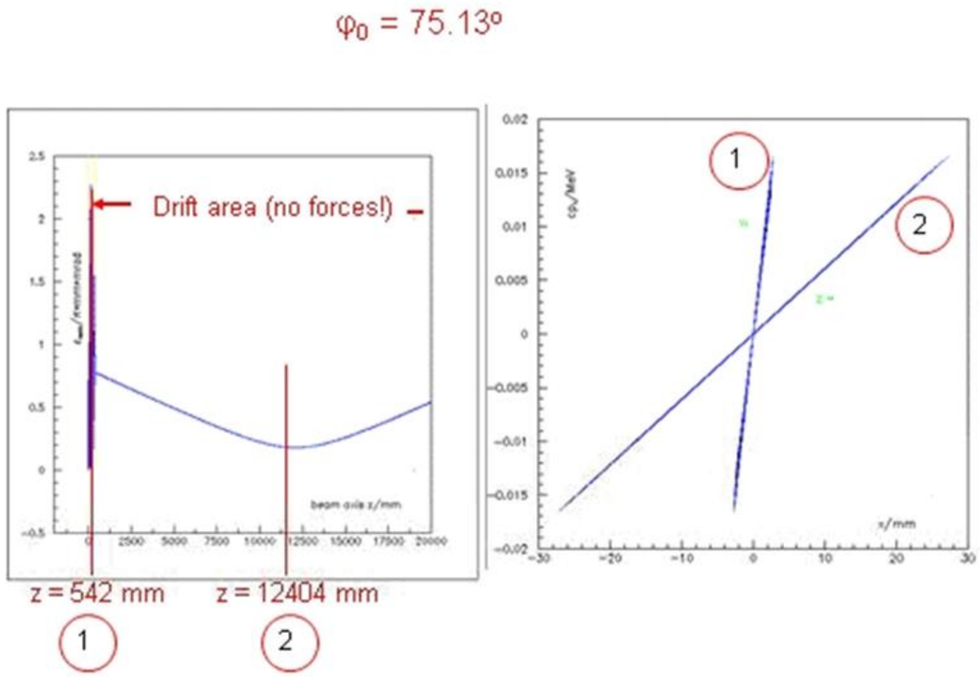

Fig.8a: Phase space plots at two z-positions in the drift area.

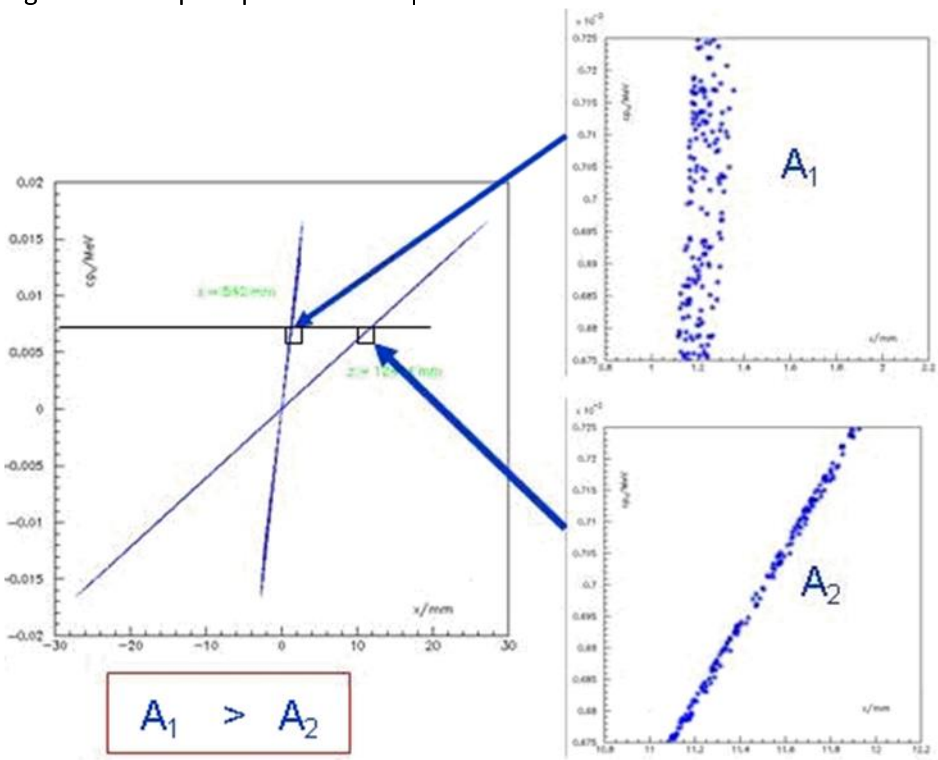

Fig. 8b: Zooming in the phase space distribution of Fig. 8a.

Fig. 8b shows the much smaller area A_2 of the phase space plot for the minimum position as compared to the area A_1 at position z_1 at the gun exit.

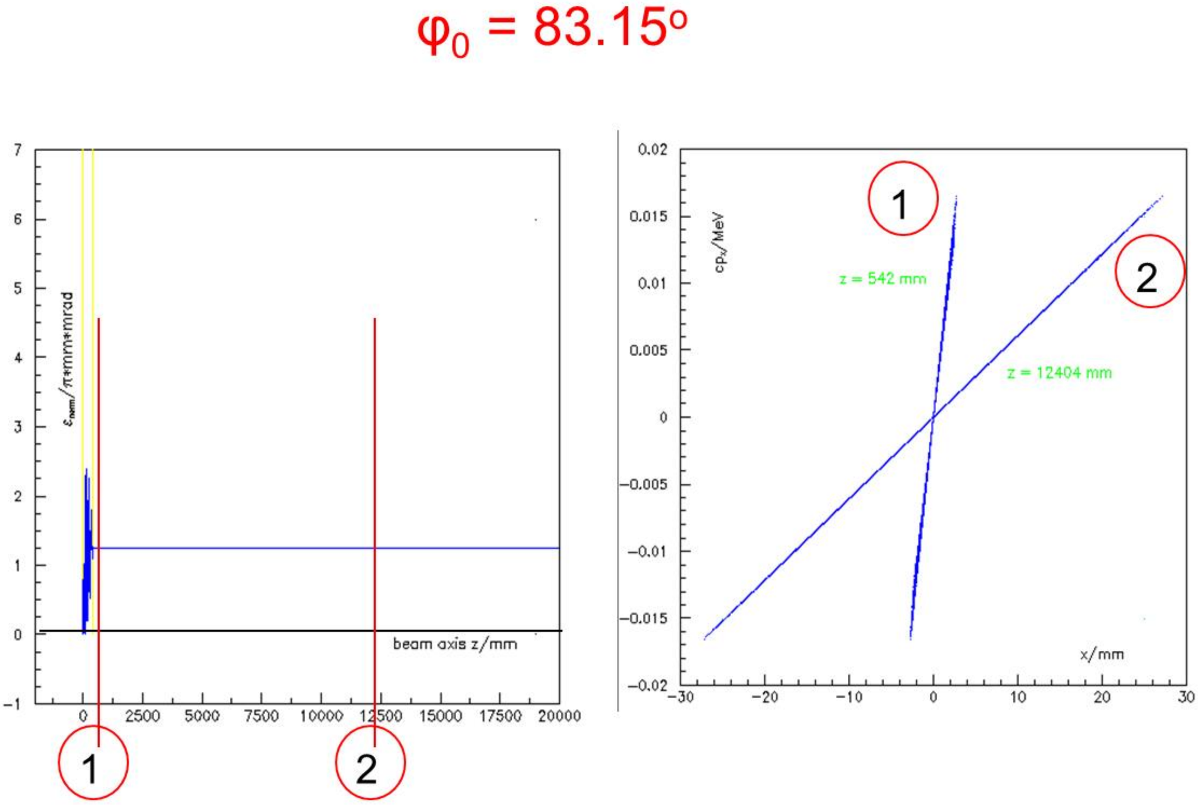

Fig.9a: Comparison of the phase plots at positions z_1 and z_2 for starting phase ϕ_{start} = 83.15°.

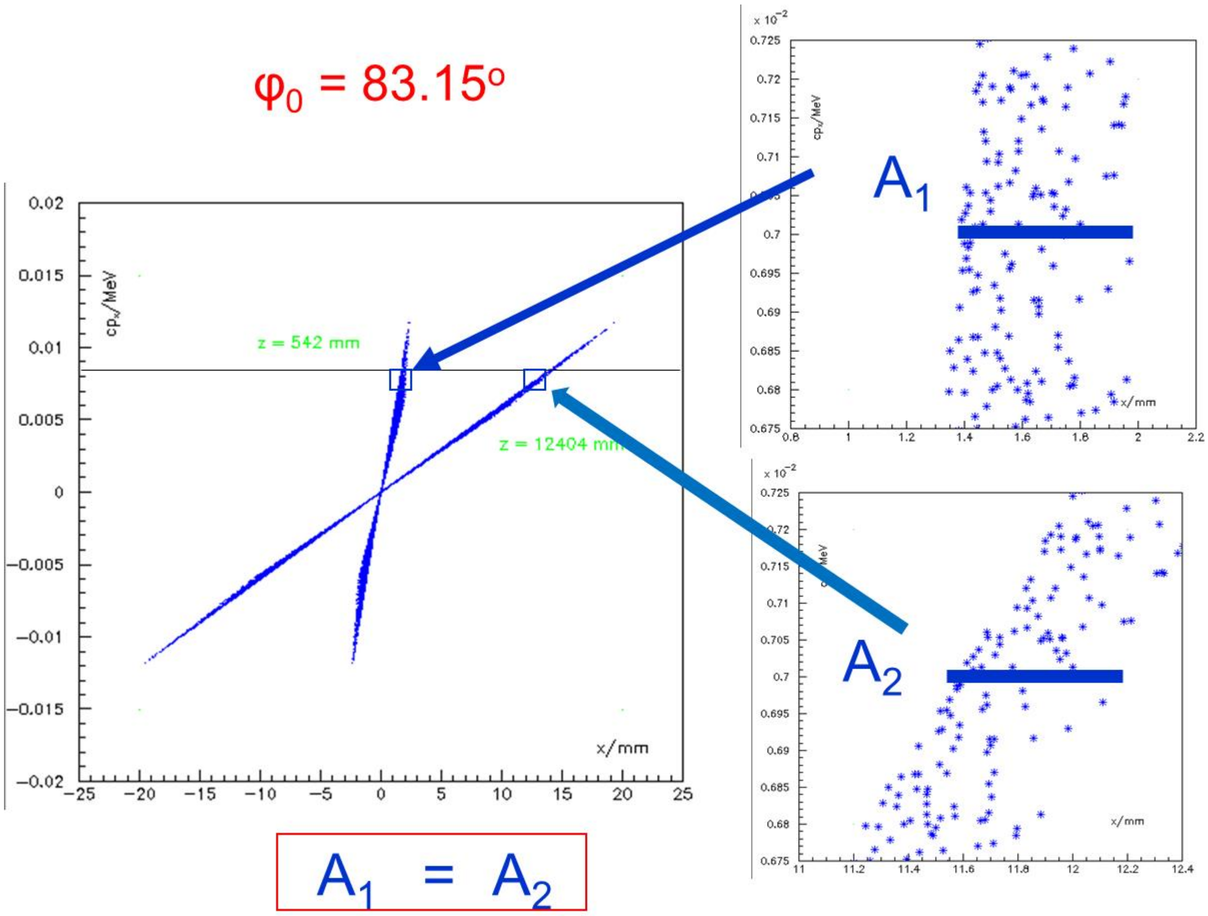

Fig.9b: Zooming in the details of Fig.9a.

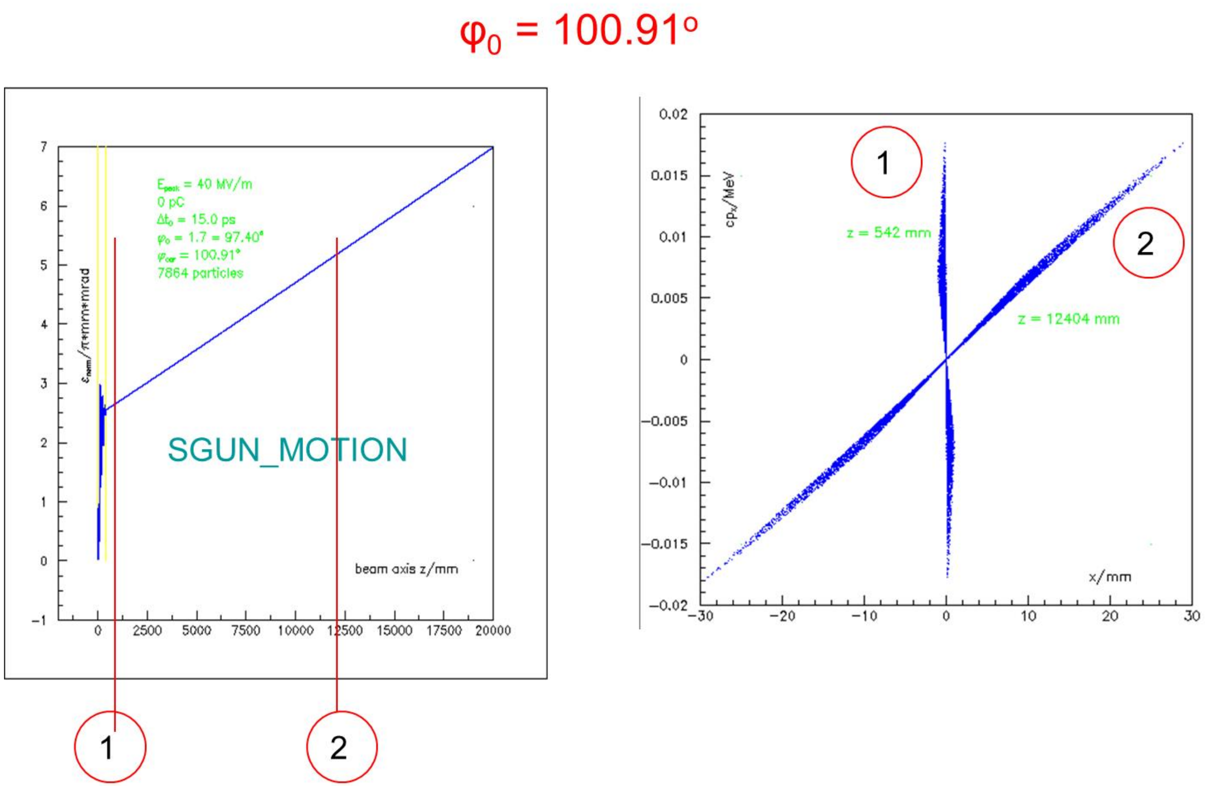

Fig.10a: Comparison of the phase plots at positions z_1 and z_2 for starting phase $\phi_{start} = 100.91^{o}$.

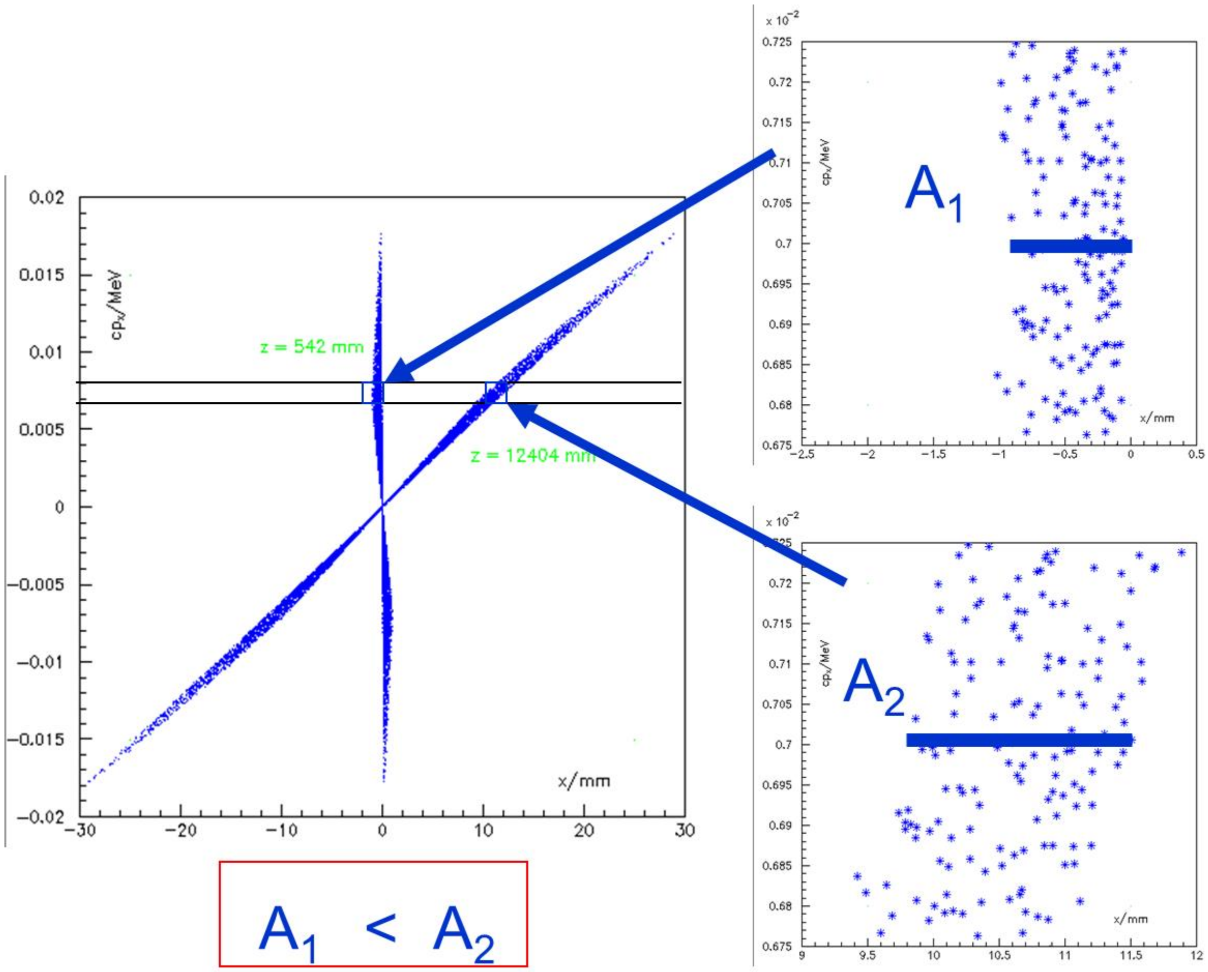

Fig.10b: Zooming in the details of Fig.10a.

Next we will study the correlations between the velocity and the position x of the particles in the phase space plots for a very small momentum channel Δp_x. Theoretically the width of this channel should be chosen equal to zero but in the simulation calculations one has to choose some finite width so that at least there are a few particles falling in this channel. The scheme is shown in fig.11 where we have 5 particles in the channel 0 $.7*10^{-2}$ MeV ≤ cp_x ≤ $0.7025*10^{-2}$ MeV.

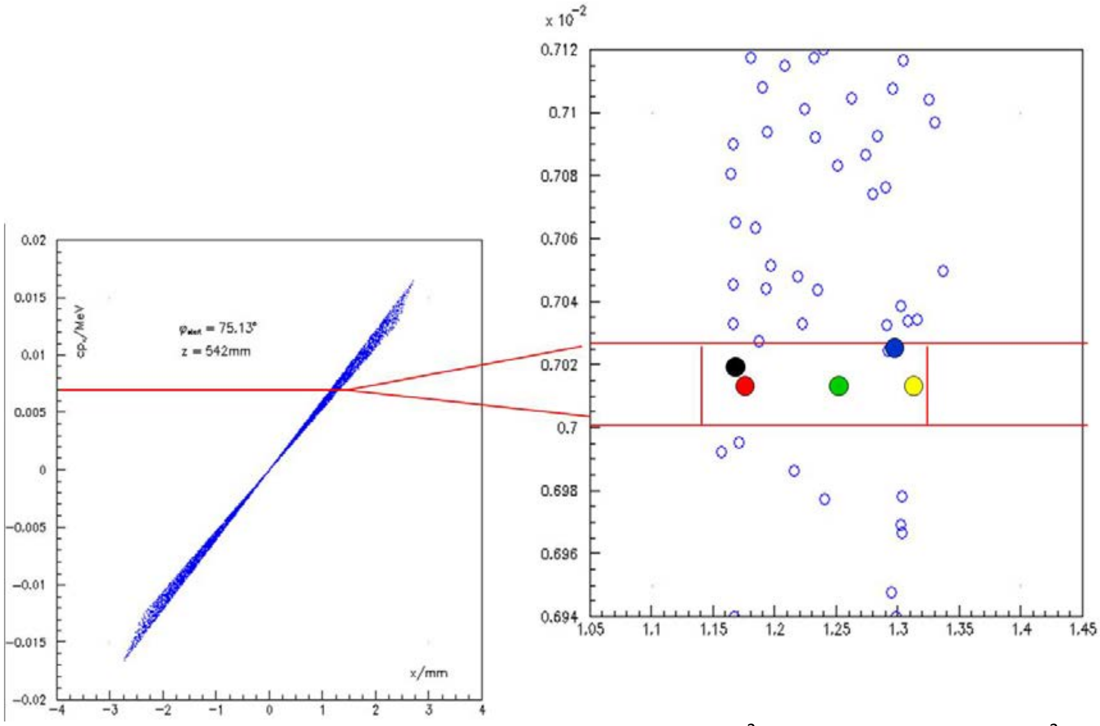

Fig.11: A small momentum channel is chosen between $0.7*10^{-2}$ MeV ≤ cp_x ≤ $0.7025*10^{-2}$ MeV to create a kind of a virtual box as demonstrated in Fig.6. The five coloured particles fall into this box.

Next in fig.12 we look at the velocity v_x-distribution for the 5 particles inside the virtual box.

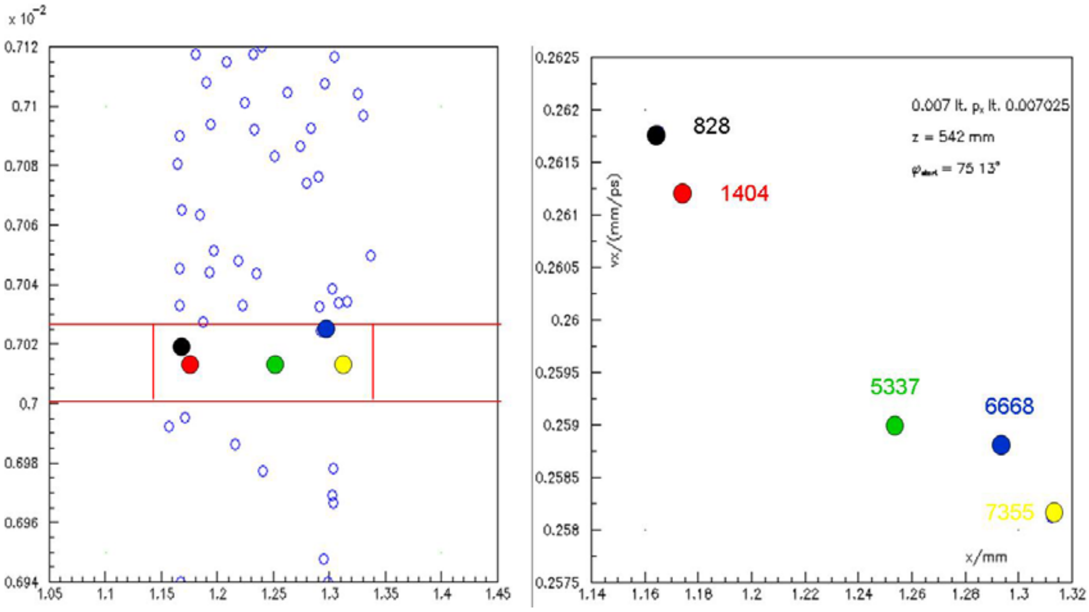

Fig.12: Velocity correlation of the particles inside the virtual box. The numbers indicated at the particles in the right-hand side picture are the respective particle numbers in the simulated bunch.

As can be seen from fig.12 there is a clear correlation between the position x of the particles in the phase space plot and the velocity v_x. The particles for smaller x-values are faster than the ones for higher x-values. This is the scenario where according to the theoretical discussion an emittance minimum is expected and where in fact a minimum is seen (fig.8a). In fig.13 we compare the velocity correlations for the 3 starting angles.

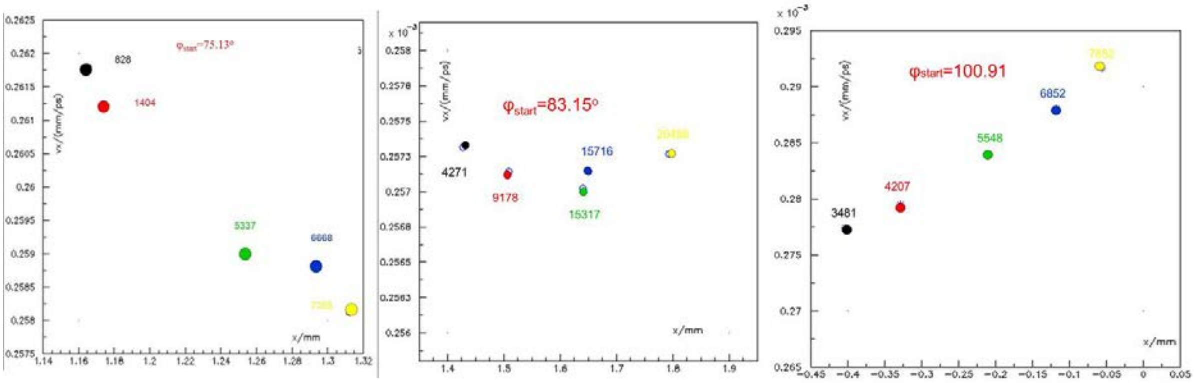

Fig.13: Correlations for the three different starting angles

The next thing to study is the correlation of the 5 particles in the chosen momentum channel with total energy. This correlation is shown in fig.14.

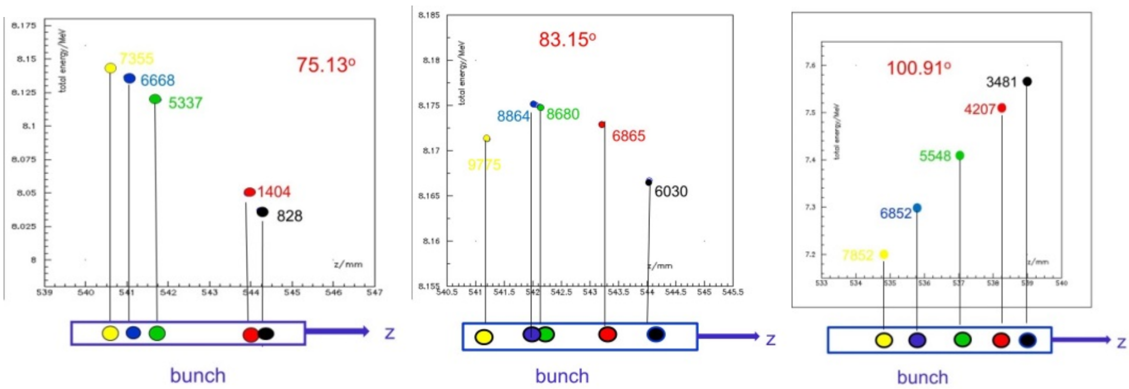

Fig.14: The correlation of the particles in the chosen momentum channel between the bunch position versus the total energy E.

One should note that according to eq. (16a) we have the relation

$$p_x = \frac{c^2}{E} v_x. \tag{17}$$

Referring to eq. (16) this is easy to understand since the 5 particles belong to the same very small momentum channel.

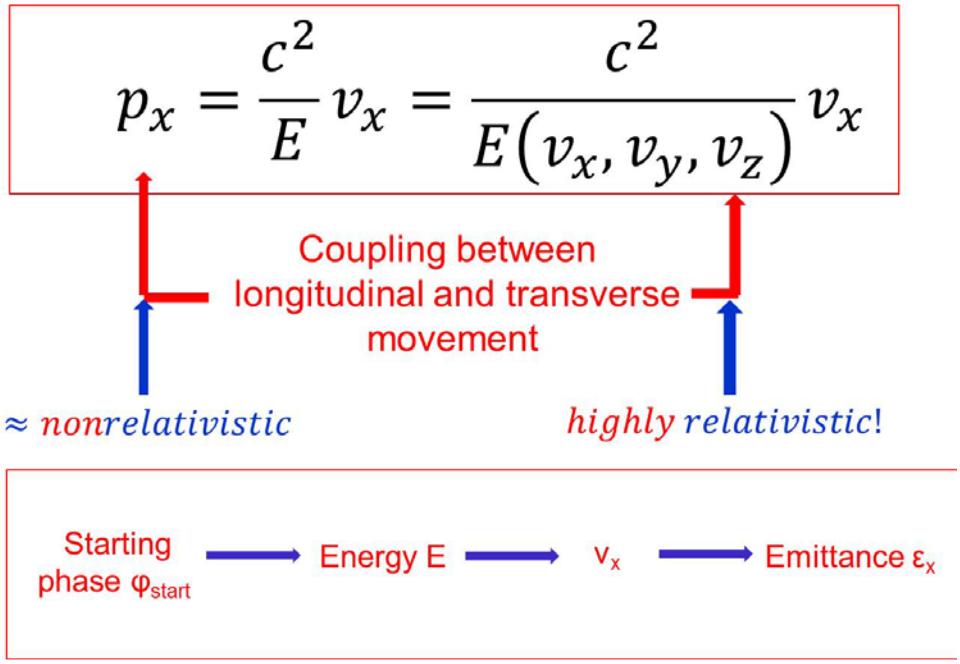

Fig.15: General coupling scheme.

Next we trace back the selected particles in the small momentum channel Δp_x to the cathode of the gun. This can be done in a second run of the simulation calculation since the particle numbers are known. In this way one is able to understand how the respective $v_x - x$ correlations come about.

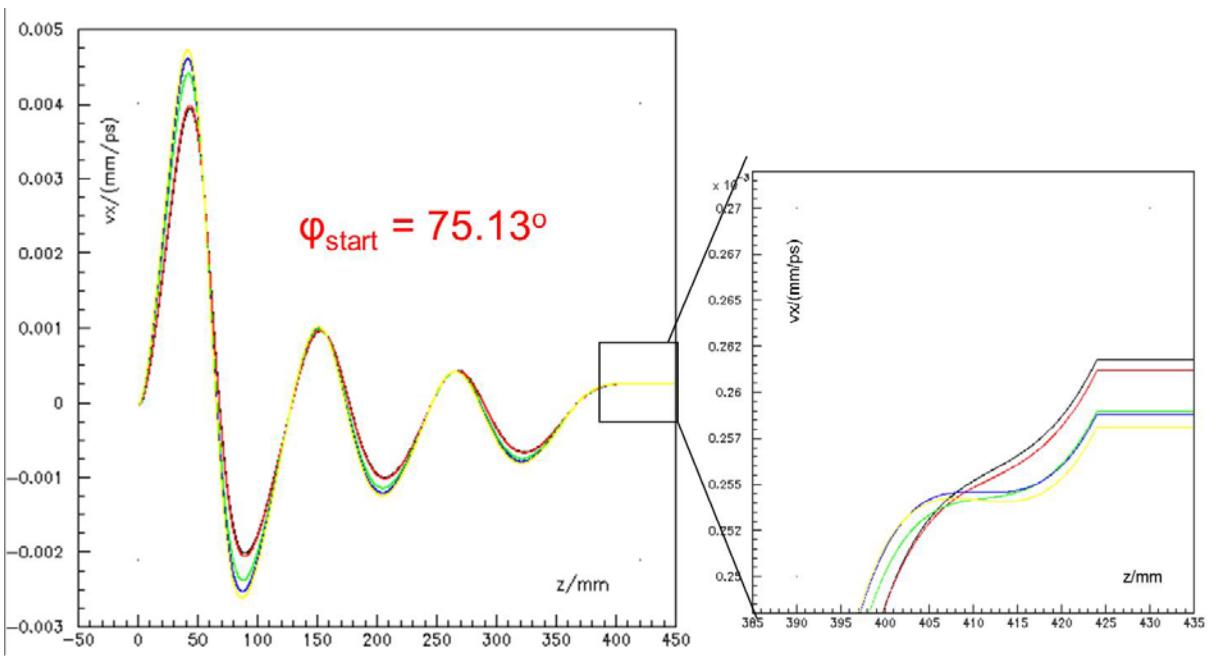

Fig. 17: The v_x behaviour of the selected particles inside the gun.

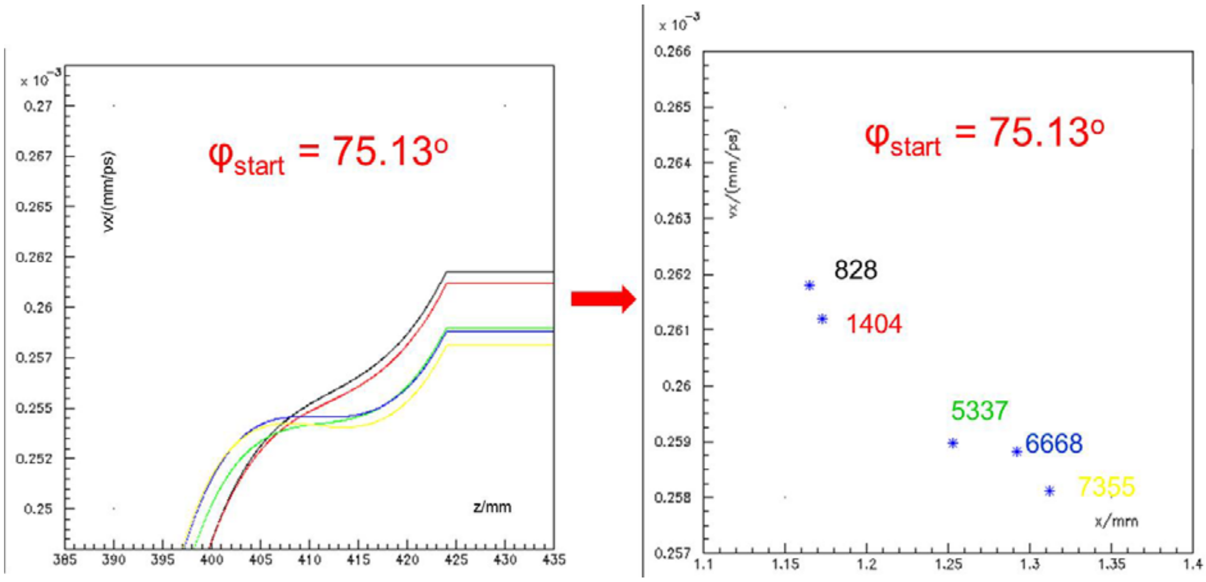

Fig.18: Detailed representation of fig.17. The velocity behaviour at the gun exit can be traced back to a cross over at z = 410 mm.

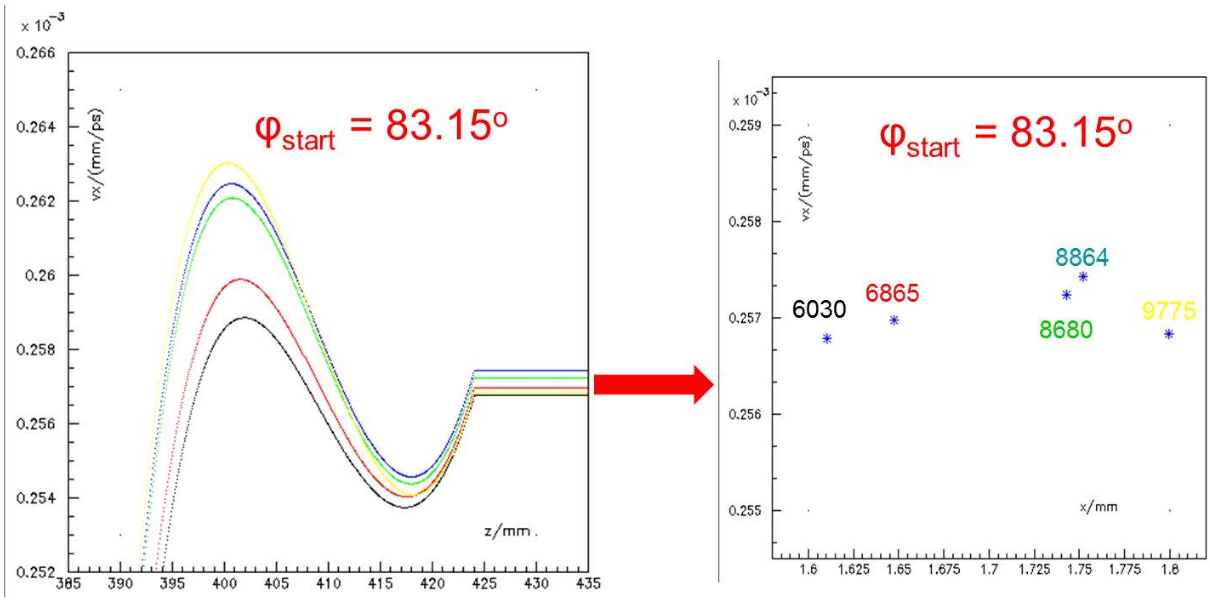

Fig.19: No cross over is observed for the constant emittance case.

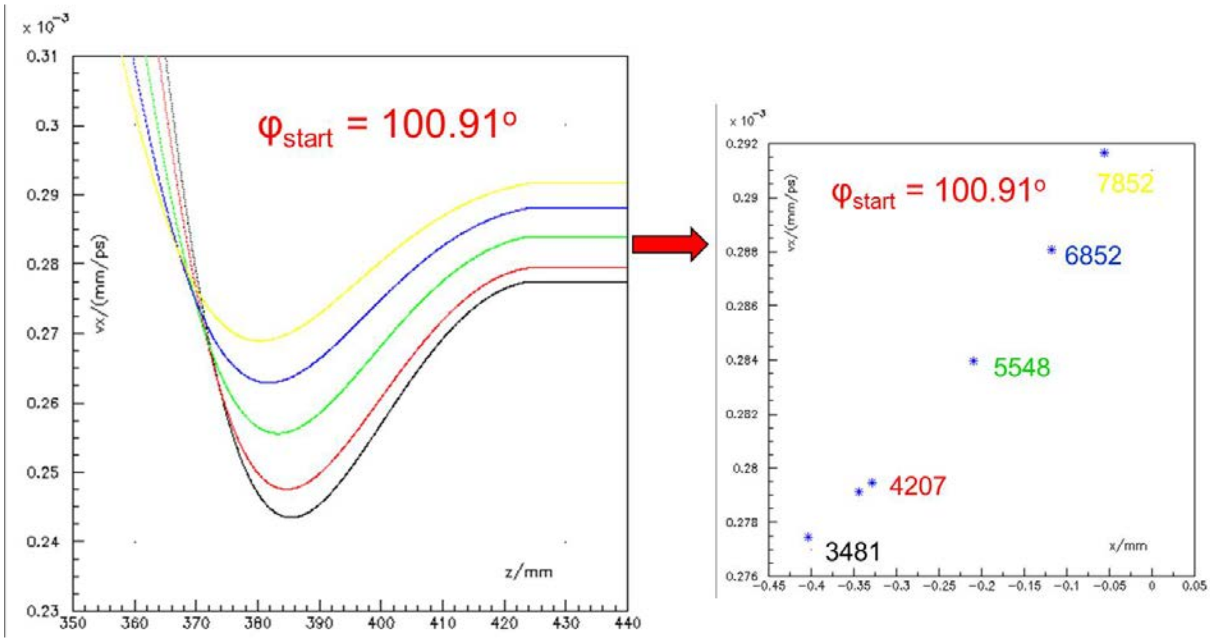

Fig. 20: For the increasing emittance case a cross over is observed at z =370 mm.

6. Emittance minimum with space charge switched on

In fig. 20 through 22 we show calculations with the space charge interaction switched on. One can see that the emittance minimum of the 0 pC case survives even at 1 nC bunch charge. But with increasing bunch charge the minimum gets shallower.

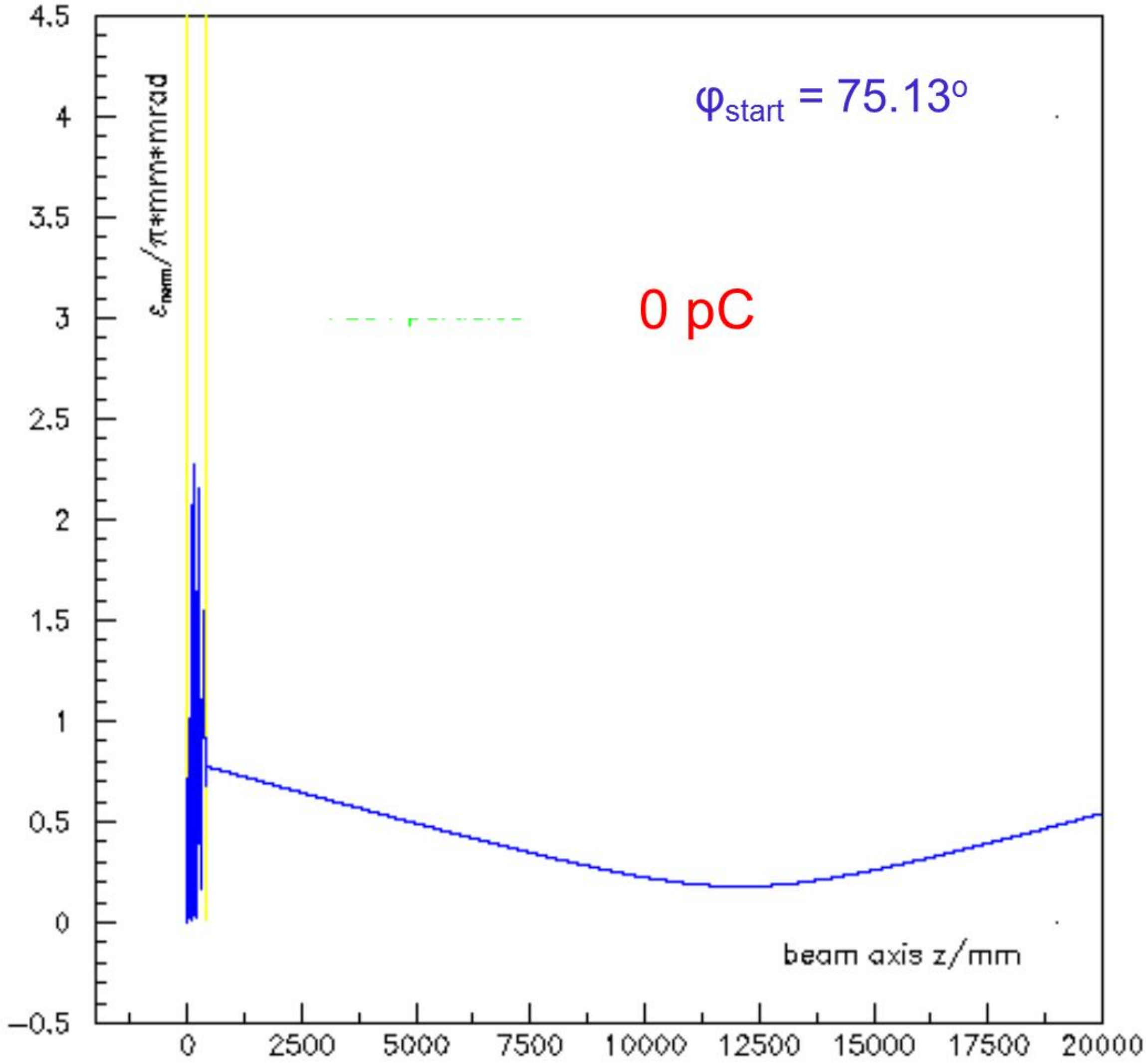

Fig. 20: Emittance minimum for 0 pC bunch charge.

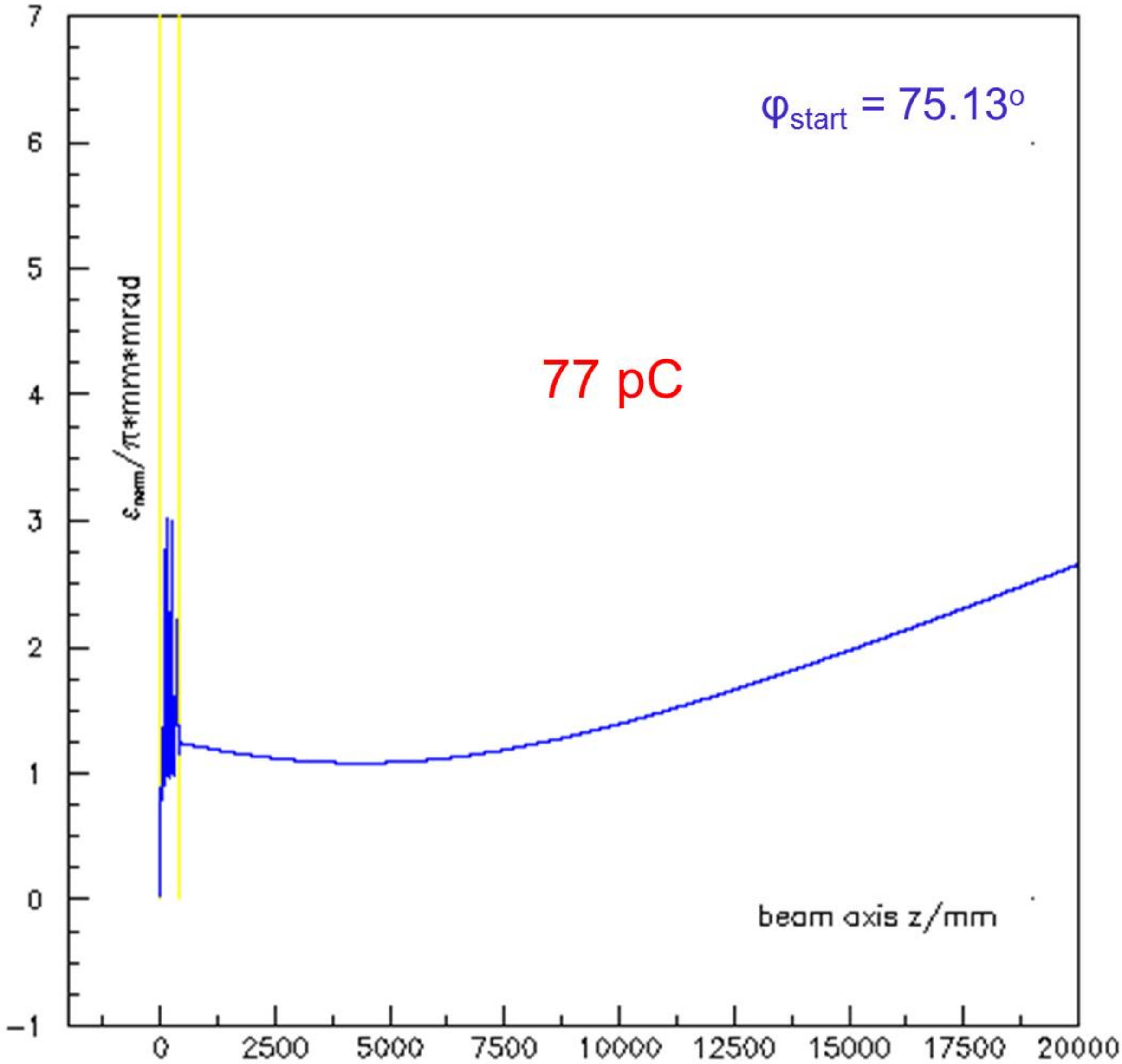

Fig.21: Emittance minimum for 77 pC bunch charge.

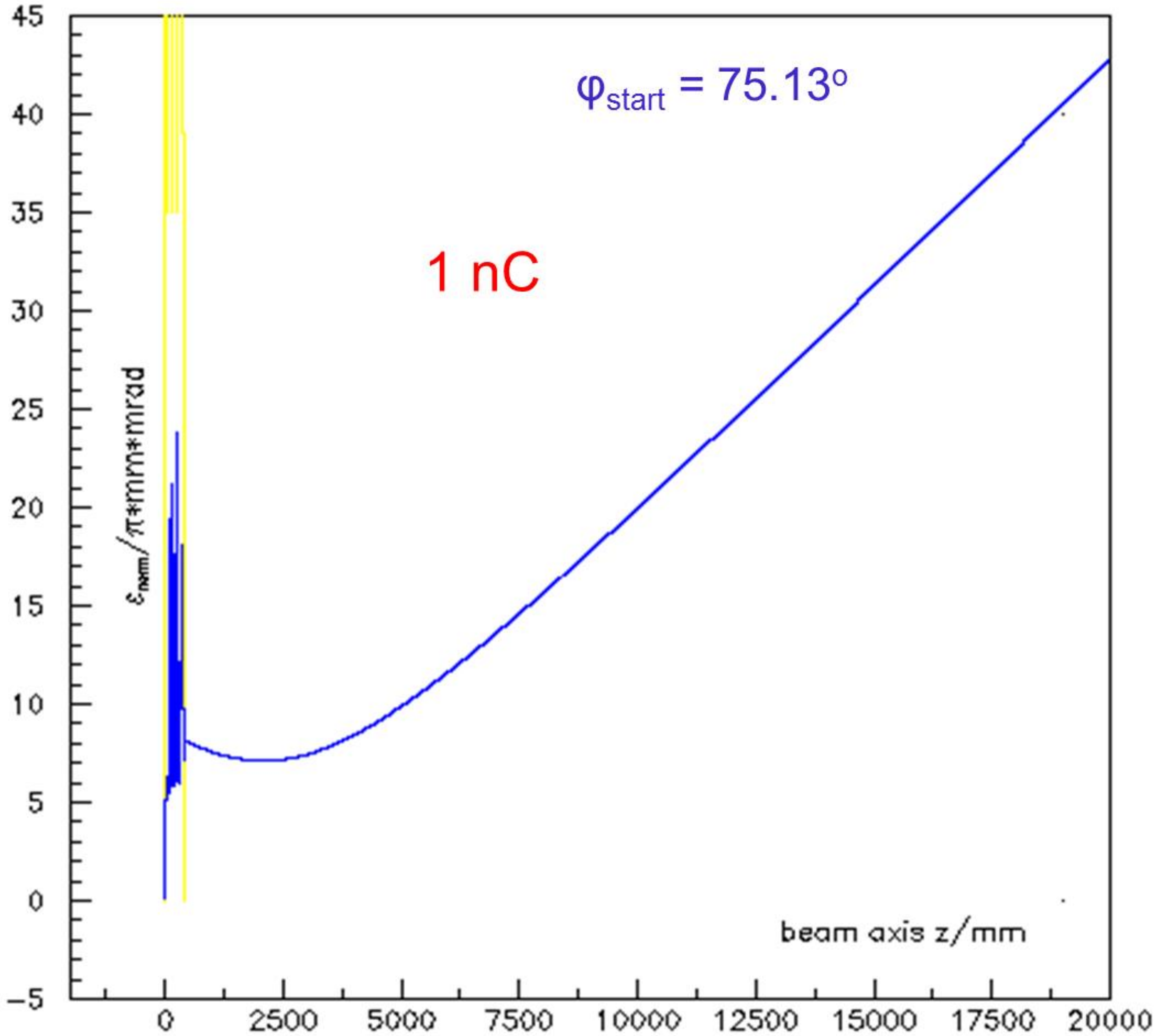

Fig. 22: Emittance minimum for 1 nC bunch charge.

References

1. A. Arnold, et al., Nuclear Instruments and Methods, A577 (2007) 440.

2. K. Moeller, "Simulation calculation of electron motion in the ELBE superconducting electron gun", Radiation Source ELBE Annual Report 2002, p. 57, report FZR-275, 2003.

3. K.Floetmann, ASTRA, http://www.desy.de/~mpyflo/Astra_dokumentation/